

Electronic Supplementary Information

Pico-HPLC system integrating equal inner diameter femtopipette into 900-nm i. d. porous layer open tubular column

Ruonan Li,[‡] Yunlong Shao,[‡] Yanmin Yu, Xiayan Wang* and Guangsheng Guo

Beijing Key Laboratory for Green Catalysis and Separation, Department of Chemistry
and Chemistry Engineering, Beijing University of Technology, Beijing 100124, China

*Corresponding author: xiayanwang@bjut.edu.cn

[‡]These authors contributed equally to this publication.

Experimental Section

Chemicals.

2-Acrylamido-2-methylpropane sulfonic acid (AMPS), butyl methacrylate (BMA), 1-propanol, 1,4-butanediol, 2-hydroxyethyl methacrylate (HEMA), ethylene glycol dimethacrylate (EDMA), 3-(trimethoxysilyl)-propyl methacrylate (γ -MAPS), 4-fluoro-7-nitro-2,1,3-benzoxadiazole (NBD-F), and DL-alanine were obtained from J&K Chemical. Ammonium persulfate (APS), 1-dodecanol, and N,N'-methylene bisacrylamide (bis) were purchased from Sigma-Aldrich (USA). DL-proline and fluorescein (disodium salt) were bought from Acros Organics. DL-serine and DL-glutamine were purchased from Tokyo Chemical Industry Co., Ltd. (Japan). *O*-9-[2-(methacryloyloxy)-ethylcarbonyl]-10,11-dihydroquinidine (MQD) was kindly provided by Professor Zhengjin Jiang from Jinan University. Trifluoroacetic acid (eluent additive for LC-MS), methanol and acetonitrile were purchased from Thermo Fisher Scientific. Methanol and acetonitrile were of HPLC grade. Disodium tetraborate decahydrate, acetone and thiourea were obtained from Beijing Chemical Works (Beijing, China). Sodium acetate anhydrous, sodium hydroxide, acetic acid glacial, acrylamide, 2,2'-azobisisobutyronitrile (AIBN) and hydrofluoric acid were obtained from Tianjin Fuchen Chemical Reagent Factory (Tianjin, China). Boric acid and ammonium formate were purchased from Sinopharm Chemical Reagent Co., Ltd. (China). Formic acid, ammonium hydroxide, cyclohexanol and N,N,N',N'-tetramethylethylenediamine (TEMED) were purchased from Tianjin Guangfu Fine Chemical Research Institute (Tianjin, China). The water in all experiments was purified using a Thermo Scientific Water Purification System. Fused silica capillaries were specially produced by Polymicro Technologies Inc (USA).

Instrument.

The voltage for sampling was supplied by Keithley 2400 Series SourceMeters. The morphology of the monolith and pico-PLOT columns was characterized using FEI Nova NanoSEM 430 Field Emission Scanning Electron Microscopy (SEM). The morphology of the porous layer of the pico-PLOT columns was analyzed using a FEI Tecnai F20 Transmission Electron Microscope (TEM). A DW-P303-1ACF0 high-voltage power source from Tianjin Dongwen high-voltage power source factory was used to test the performance of the EOP monolith.

Setup of the pico-HPLC.

The pico-HPLC system was coupled with an LIF detector (Fig. S1). A 54.5-cm pico-PLOT column with a femtopipette tip served as the sampler and enantioseparation column. The sample was detected on-column using a custom LIF detector, as explained in our previous report.¹ Data were collected using Labview software. The end of the pico-PLOT column was connected to a 23.8-cm EOP monolith by a PEEK tee. The third outlet of the tee joint was connected to a bubbleless electrode with a length of 2.3 cm. The other ends of the monolith and the electrode were inserted into buffer reservoirs. High voltage was applied to electrode 1 when the system was sampling.

After sampling, the EOP monolith and bubbleless electrode were removed, and the femtopipette was transferred to a buffer vial. Nitrogen was introduced into the chamber to drive the buffer solution or sample solution into the pico-PLOT column.

Preparation of chiral pico-PLOT column with femtopipette tip.

A capillary with a 900-nm i.d. was first activated by 1 mol L⁻¹ NaOH solution for 5 h and subsequently washed with water for 3 h. After flushed with acetone, the capillary was dried using nitrogen. Then, the capillary, which was filled with a mixture of γ -MAPS and acetone (v/v=1), was stored in the dark for 24 h. Subsequently, the capillary was washed with acetone and dried with N₂. The porous layer of the PLOT column was prepared according to the literature with some modification.² A polymerization solution of 3.98% MQD, 7.92% HEMA, 7.98% EDMA, 39.77% cyclohexanol, 40.00% 1-dodecanol and 0.35% AIBN was vibrated and ultrasonically mixed. After purging with N₂, the solution was introduced into the capillary. Both ends of the capillary were sealed with septa after the capillary was filled with the polymerization mixture. The last 6 cm at each end of the capillary, which were used as the detection window for LIF or to fabricate the femtopipette, were filled with air. The solution was polymerized at 60 °C for 2 h. The residual solution in the pico-PLOT column was rinsed with methanol using the LC pump. All solutions for fabrication were filtered through a 0.22- μ m pore membrane before use.

Approximately 2 cm of the polyimide polymer coating was peeled off to expose the fused silica, which acted as an etching window at a distance of 4 cm from the end of the pico-PLOT column to prepare the femtopipette. The pico-PLOT column was inserted into a 200- μ m i.d. bare capillary vertically and adhered to the capillary using paraffin wax (Fig. S2). Both the fused silica and sleeving capillary were vertically immersed in 40% hydrofluoric acid (HF) for ~1 h at 30 °C (Fig. S2). The pico-PLOT was aerated with N₂ to prevent the inner wall from etching. The femtopipette tip was obtained when the fused silica fractured. After etching, the femtopipette was washed thoroughly with deionized water and dried under N₂.

Preparation of EOP monolith and bubbleless electrode.

The EOP monolith and bubbleless electrode were prepared in capillaries with an i.d. of 100 μ m according to reported protocols.³

In brief, the 100- μ m i.d. capillaries were sequentially flushed with 1 mol L⁻¹ NaOH, water, acetone and N₂. Then, the capillaries were filled with a mixture of 50% γ -MAPS and 50% acetone(v/v) and left in the dark for 24 h. After modification, the capillaries were washed with acetone and dried with N₂. Subsequently, the capillaries were used to prepare the EOP monolith and bubbleless electrode.

A mixture of 1% AMPS, 22.91% BMA, 15.94% EDMA, 41.36% 1-propanol, 12.41% 1,4-butanediol, 5.98% water and 0.40% AIBN was introduced into the capillaries. Then, the capillaries were sealed with septa and stored in a 60 °C water bath for 20 h. After polymerization, the monolith columns were rinsed with methanol.

For the bubbleless electrode, 1 mL of 15%T (%T is the weight concentration of bis and acrylamide) and 2% C (% C is the bis concentration relative to acrylamide), 2 μL of 100% TEMED and 20 μL of 10% APS (weight concentration) were introduced into the capillaries and stored at 0 °C overnight, followed by storage at 4 °C for 24 h. The monolith and bubbleless electrode were stored in 3 mmol L⁻¹ sodium acetate solution.

Construction and characterization of EOP.

The EOP was assembled using a negatively charged polymer monolith and a bubbleless electrode as described previously with some modifications.⁴ In brief, one end of the monolith, which was filled with 3 mmol L⁻¹ sodium acetate solution, was connected with a bubbleless electrode and a bare capillary with an inner diameter of 50 μm via a PEEK tee. The bubbleless electrode was inserted into the cathode reservoir, and the other end of the monolith was inserted into the anode reservoir. The length of the monolith was 26.10 cm. The pumping pressure was measured after the high voltage was applied.

The monolith was cut into 5-mm lengths for analysis by SEM imaging. The electroosmotic mobility was determined using a capillary electrophoresis system with an ultraviolet (UV) detector. A detection window was burned at a distance of 5 cm from the cathode reservoir. The sampling end of the monolith was placed in the anode reservoir. Then, 5 mmol L⁻¹ thiourea was injected at 5 kV for 3 s and detected at 214 nm. The pumping solution was driven by 5 kV.

Characterization the femtopipette of the pico-HPLC system.

A standard curve for fluorescein from 1 pmol L⁻¹ to 200 nmol L⁻¹ was constructed to calibrate the volume that was aspirated by the femtopipette of the bifunctional chromatographic column. The monolith and bubbleless electrode were protected in 3 mmol L⁻¹ sodium acetate solution before use. The pico-PLOT column was prefilled with the buffer solution for enantioseparation before assembly with an EOP monolith and a bubbleless electrode via a PEEK tee. The monolith with a length of 23.80 cm and the bubbleless electrode with a length of 2.30 cm were inserted into the solution reservoirs, which were filled with 3 mmol L⁻¹ sodium acetate solution. The femtopipette was placed in a 2.0 mmol L⁻¹ sodium tetraborate solution that contained 2.5 mmol L⁻¹ fluorescein. First, a high voltage was applied on electrode 1 to drive the EOP pump to aspirate a small volume of fluorescein solution. The volume of aspirated fluorescein solution was controlled using the aspiration time and applied voltage. Then, the outer wall of the femtopipette was washed with 2.0 mmol L⁻¹ sodium tetraborate solution quickly. A high voltage was subsequently applied to electrode 2 to push the solution into a vial containing 25 μL of 2.0 mmol L⁻¹ sodium tetraborate solution. The time to push the solution must be a little longer than the suction time. Then, the femtopipette was washed three times before the next sampling. The solutions with different volumes of fluorescein solution were detected using LIF.

Derivatization of amino acids and chromatographic conditions.

The amino acid enantiomers were derivatized with NBD-F. Briefly, 100 μL of 20 mmol L^{-1} NBD-F dissolved in acetonitrile was added to a mixture of 400 μL of 1 mg mL^{-1} amino acid enantiomers and 100 μL of 40 mmol L^{-1} sodium–borate buffer (pH 8.0) and maintained at 65 $^{\circ}\text{C}$ for 4 min. Finally, 950 μL of 2%(v/v) TFA in H_2O was added to the reaction mixture.

All solutions in the pico-HPLC system were filtered through a 0.22- μm membrane. The total length and effective length of the column for separating NBD-derivatized amino acids were 54.55 cm and 49.15 cm, respectively. The NBD-derivatized proline enantiomers and serine enantiomers were introduced using the femtopipette with a driving voltage of 0.1 V for 9 s, whereas the NBD-derivatized alanine enantiomers and glutamine enantiomers were sampled at 0.1 V for 4 s. The mobile phase, which was composed of 80% acetonitrile and 0.1 mol L^{-1} ammonium formate solution with an apparent pH of 6.0, was driven by a pressure of 1000 psi. A flow rate of 13.50 pL min^{-1} was applied to separate the NBD-derivatized amino acid enantiomers.

Computational Method.

All calculations were accomplished based on Dreiding force field⁵ using Forcite module in Materials Studio v6.1. Molecular dynamics simulations and molecular mechanics method were combined to search low energy conformation of the interaction structures between MQD and NBD-derivatized amino acid enantiomers. Molecular dynamics simulation was performed in the canonical ensemble. The temperature was maintained at 298 K, and the total simulation time amounted to 5 ns. The Charges of atoms in molecules were assigned and calculated according to charge equilibration (QEq) method.⁶

The intermolecular interaction energies between NBD-derivatized amino acid enantiomers and MQD were calculated according to the equation:

$$\Delta E_{\text{inter}} = (E_{\text{MQD}} + E_{\text{enantiomer}}) - E_{\text{enantiomer-MQD}} \quad (1)$$

Where E_{MQD} and $E_{\text{enantiomer}}$ are the nonbonded interaction energies of MQD and NBD-amino acid enantiomer, respectively. $E_{\text{enantiomer-MQD}}$ is the nonbonded interaction energy of the interaction structure of NBD-amino acid enantiomer with MQD, ΔE_{inter} is the intermolecular interaction energy between NBD-amino acid enantiomer and MQD, which consists of van der Waals interaction energy (ΔE_{vdw}), electrostatic interaction energy (ΔE_{elec}) and hydrogen bond interaction energy (ΔE_{hb}).

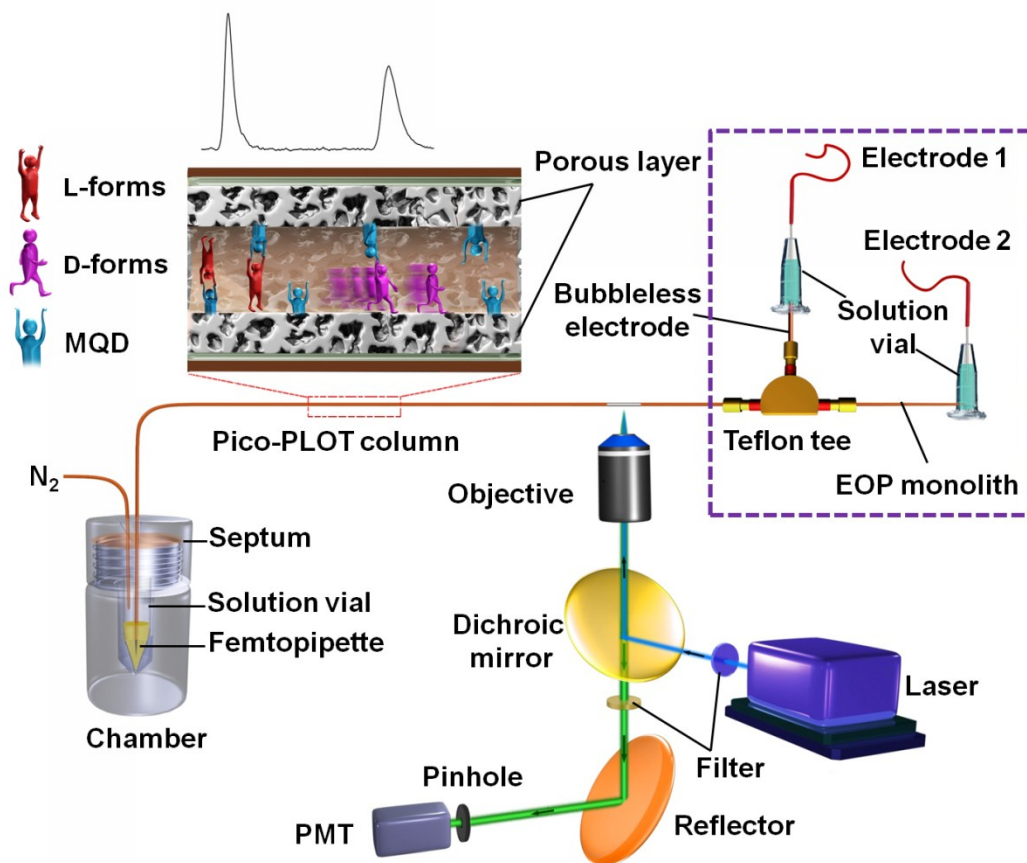


Fig. S1 The Setup of the pico-HPLC-LIF system.

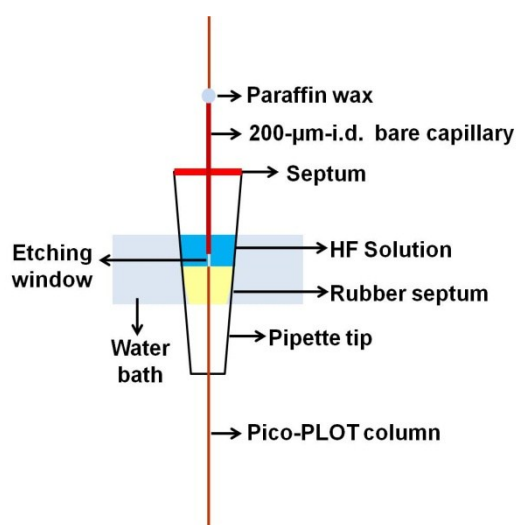


Fig. S2 The device for etching of femtopipette.

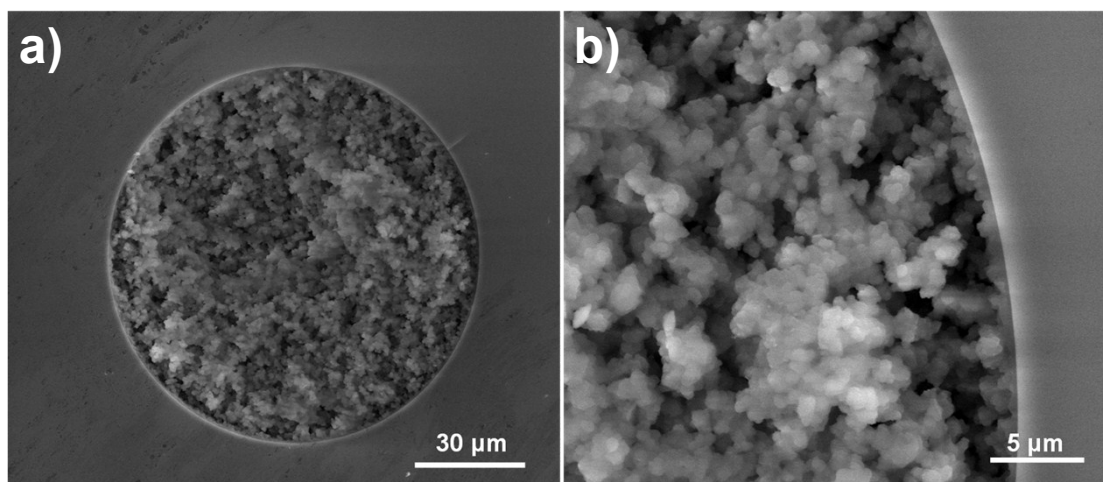


Fig. S3 SEM images of the negatively charged monolith of EOP.

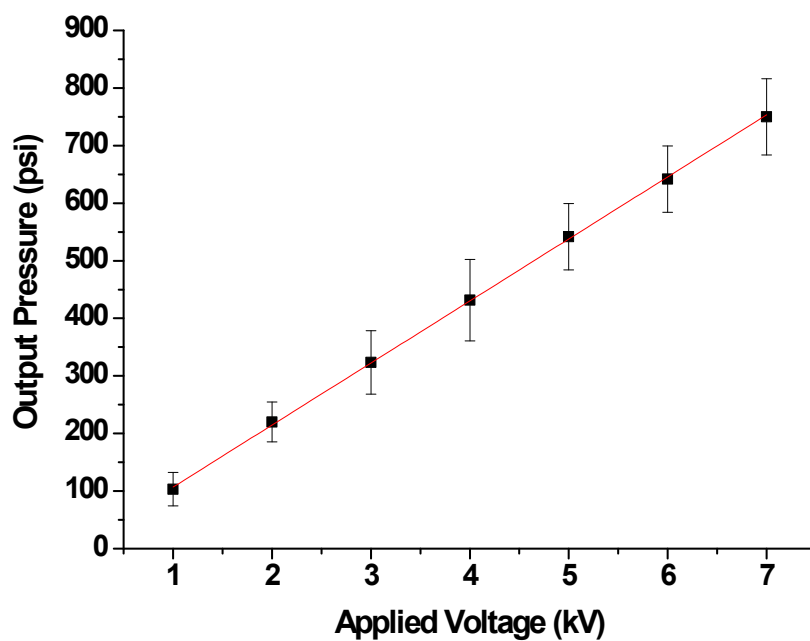


Fig. S4 Relationship between the output pressure and applied voltage. The negatively charged monolith had a length of 26.10 cm. The pumping solution was 3 mmol L⁻¹ sodium acetate (pH 5.0).

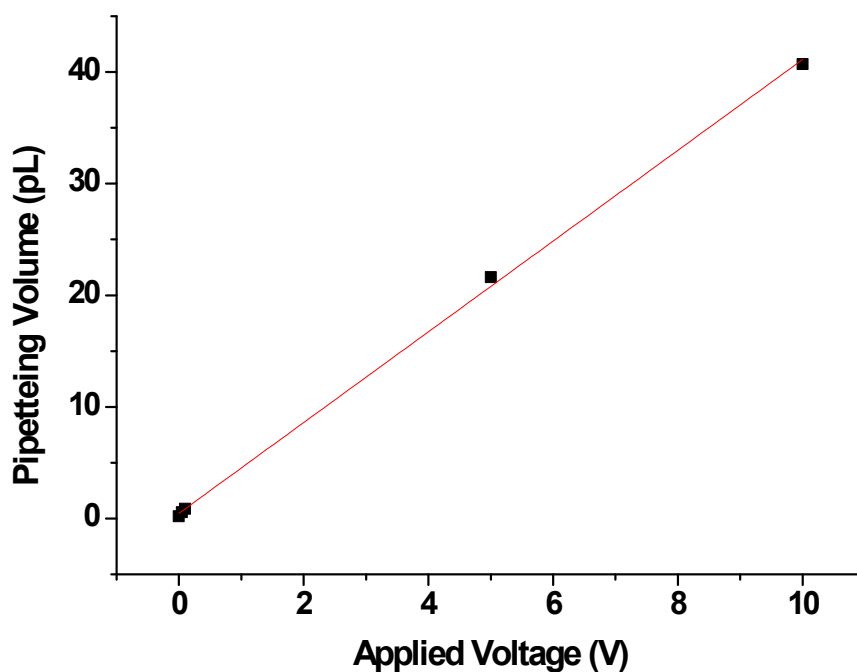


Fig. S5 Relationship between pipetteing volume and applied voltage. The sampling time is 10 s.

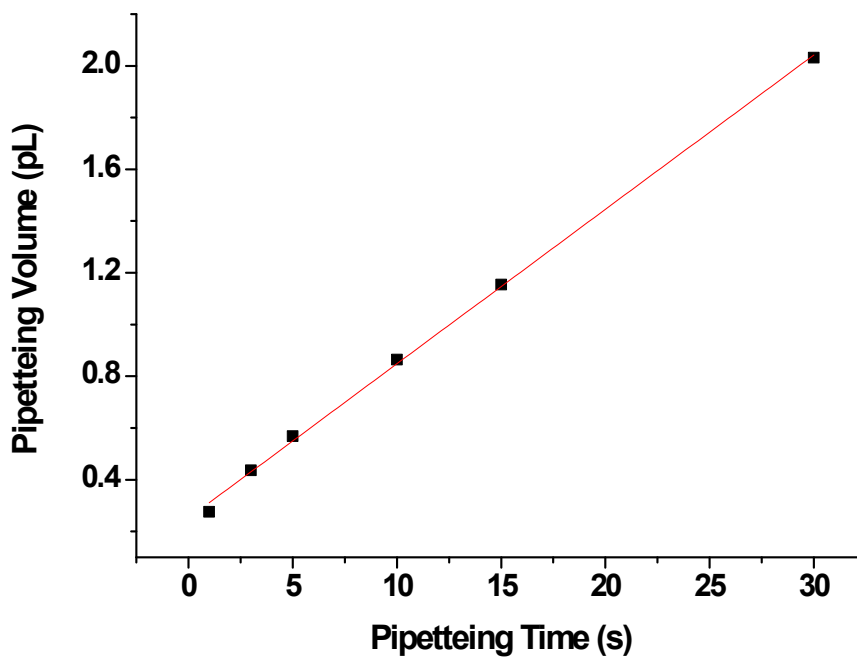


Fig. S6 Relationship between pipetteing volume and pipetteing time. The sampling voltage is 100 mV.

Table S1 Enantioseparation of NBD-derivatized amino acid enantiomers.

Sample	Sample Volume / μL	Flow Rate / $\mu\text{L min}^{-1}$	R	N_D / m^{-1}	N_L / m^{-1}
NBD-DL-alanine	490	13.50	1.9	32083	28901
NBD-DL-glutamine	490	13.50	2.3	25063	19145
NBD-DL-proline	780	13.50	6.8	154711	58845
NBD-DL-serine	780	13.50	1.8	49888	53092

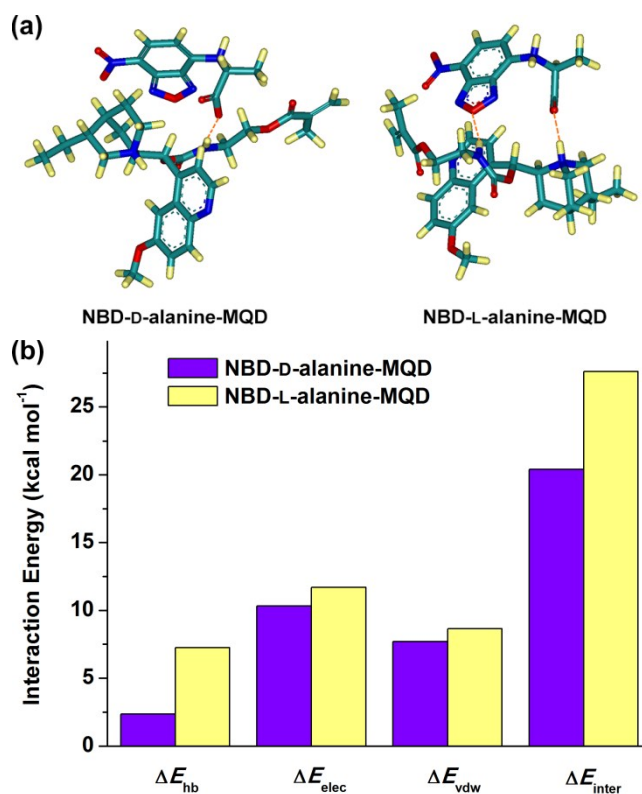


Fig. S7 (a) The interaction structures of NBD-DL-alanine with MQD. The orange dashed line represents hydrogen bond. (b) The intermolecular interaction energies between MQD and NBD-alanine enantiomers.

The difference of hydrogen bond interaction energy between NBD-D-alanine with MQD and NBD-L-alanine with MQD is the primary contribution to the difference of the interaction energies. The interaction between MQD and NBD-L-alanine includes

one additional hydrogen bond.

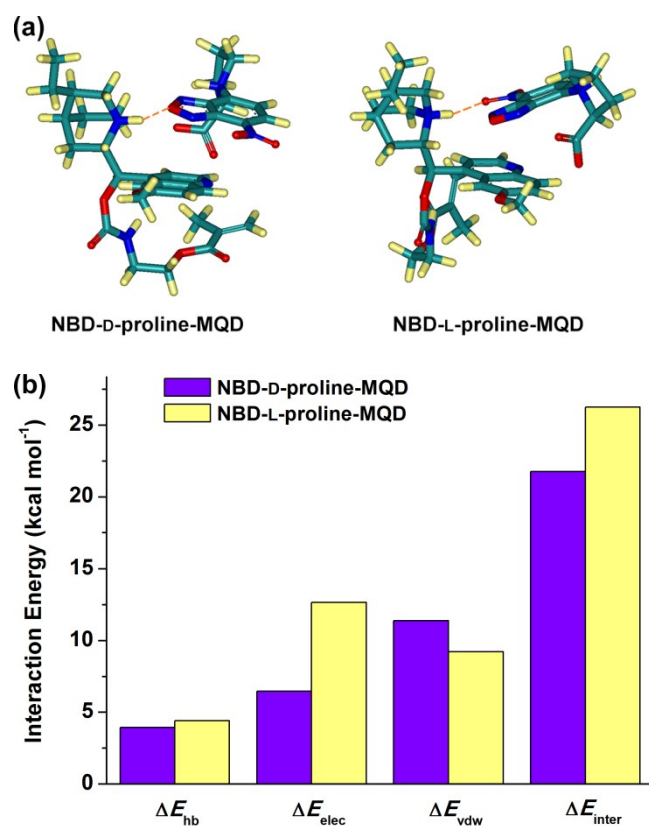


Fig. S8 (a) The interaction structures of NBD-DL-proline with MQD. The orange dashed line represents hydrogen bond. (b) The intermolecular interaction energies between MQD and NBD-proline enantiomers.

For NBD-derivatized proline, the large difference of electrostatic interaction energy between D-form and L-form with MQD plays a crucial role on the difference of intermolecular interaction energies. Two different interaction sites are observed in the interaction structures. The electrostatic interaction between L-form and MQD is stronger than the interaction between D-form and MQD.

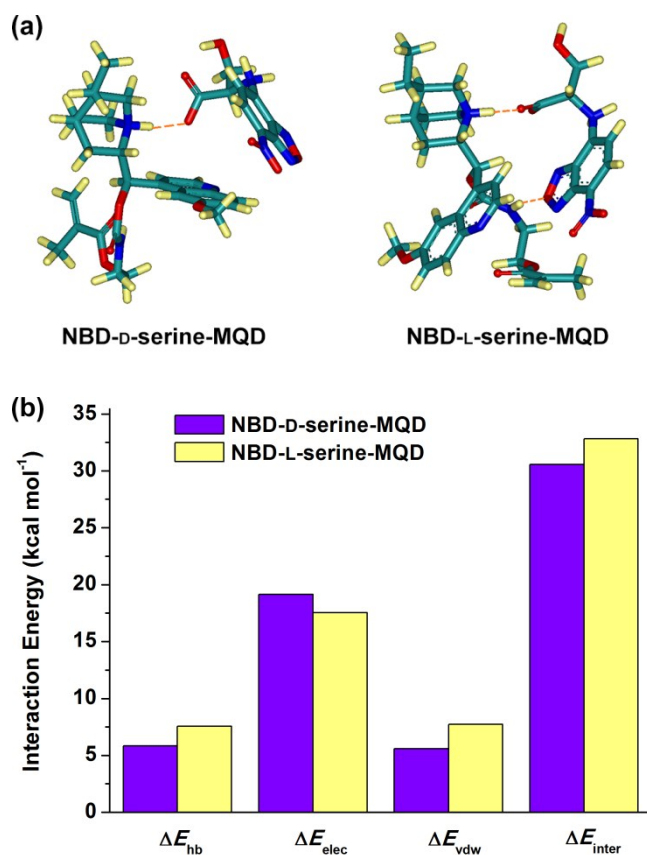


Fig. S9 (a) The interaction structures of NBD-DL-serine with MQD. The orange dashed line represents hydrogen bond. (b) The intermolecular interaction energies between MQD and NBD-serine enantiomers.

For NBD-serine enantiomers, the bar graph indicates that the electrostatic interaction of enantiomers on MQD significantly contributes to the intermolecular interaction.

References

- 1 L. Liu, V. Veerappan, Y. Bian, G. Guo and X. Wang, *Sci. China: Chem.*, 2015, **58**, 1605
- 2 Q. Wang, J. Feng, H. Han, P. Zhu, H. Wu, M. L. Marina, J. Crommen and Z. Jiang, *J. Chromatogr. A*, 2014, **1363**, 207
- 3 C. Gu, Z. Jia, Z. Zhu, C. He, W. Wang, A. Morgan, J. J. Lu and S. Liu, *Anal. Chem.*, 2012, **84**, 9609
- 4 P. Wang, Z. Chen and H.-C. Chang, *Sens. Actuators, B*, 2006, **113**, 500
- 5 S. L. Mayo, B. D. Olafson and W. A. Goddard III, *J. Phys. Chem.*, 1990, **94**, 8897

A. K. Rappé and W. A. Goddard III, *J. Phys. Chem.*, 1991, **95**, 3358